In-depth Assessment of an Interactive Graph-based Approach for the Segmentation for Pancreatic Metastasis in Ultrasound Acquisitions of the Liver with two Specialists in Internal Medicine

Jan Egger, Dieter Schmalstieg
Institute for Computer Graphics and Vision
Graz University of Technology
Graz, Austria

Xiaojun Chen
School of Mechanical Engineering
Shanghai Jiao Tong University
Shanghai, China

Jan Egger
BioTechMed-Graz
Graz, Austria
egger@tugraz.at

Lucas Bettac, Mark Hänle, Alexander Hann
Dept. of Internal Medicine I
Ulm University
Ulm, Germany

Tilmann Gräter
Dept. of Diagnostic and Interventional Radiology
Ulm University
Ulm, Germany

Wolfram G. Zoller, Alexander Hann
Dept. of Internal Medicine and Gastroenterology
Katharinenhospital
Stuttgart, Germany

Abstract— **The manual outlining of hepatic metastasis in (US) ultrasound acquisitions from patients suffering from pancreatic cancer is common practice. However, such pure manual measurements are often very time consuming, and the results repeatedly differ between the raters. In this contribution, we study the in-depth assessment of an interactive graph-based approach for the segmentation for pancreatic metastasis in US images of the liver with two specialists in Internal Medicine. Thereby, evaluating the approach with over one hundred different acquisitions of metastases. The two physicians or the algorithm had never assessed the acquisitions before the evaluation. In summary, the physicians first performed a pure manual outlining followed by an algorithmic segmentation over one month later. As a result, the experts satisfied in up to ninety percent of algorithmic segmentation results. Furthermore, the algorithmic segmentation was much faster than manual outlining and achieved a median Dice Similarity Coefficient (DSC) of over eighty percent. Ultimately, the algorithm enables a fast and accurate segmentation of liver metastasis in clinical US images, which can support the manual outlining in daily practice.**

Index Terms— **Interactive, Graph-based, Segmentation, Ultrasound, Evaluation.**

I. INTRODUCTION

With a survival rate of less than 7%, five years after diagnosis, pancreatic adenocarcinoma (PDAC) has a poor prognosis [1] and is anticipated to become the second most common cause of cancer death in 2030 [2]. In addition, most of the patients are diagnosed when they have already reached a metastatic stage [3]. However, in recent years, new therapeutic options were introduced prolong survival of patients diagnosed in a metastatic state [4], [5] and second line therapies can also increase the duration of treatment [6]-[9]. Regarding these facts, the neuroendocrine neoplasms (NEN), which is the second most common carcinoma arising from the pancreas, have also a poor prognosis when diagnosed with liver metastasis [10]. The number of staging examinations and chemotherapy cycles of these patients, which are in general performed about every two to three months, is also increasing [11] and in that context ultrasound offers a cheap and fast method to visualize focal liver lesions (FLL). Overall, ultrasound enables a similar sensitivity regarding FLL when compared with Magnetic Resonance Imaging (MRI) and Computed Tomography (CT). Moreover, ultrasound is more widespread than MRI or CT and also included as the imaging modality of choice in the German guideline for follow up of patients after resection of stage I or II colon cancer [12]. Additionally, ultrasound is recommended for the response evaluation of pancreatic cancer patients undergoing palliative treatment by the ESMO-ESDO clinical practice guidelines [13]. However, because of the different appearances of liver metastasis in ultrasound images acquisitions, the interpretation of these have a poor inter-observer agreement [14], [15]. Finally, the manual outlining of liver lesions to assess their size is time- consuming and yields to different results due to the poor inter-observer agreement.

Others working in the segmentation [16]-[21] area of US images, are for example Hao et al. [22], Bahrami et al. [23], Bakas et al. [24], Gatos et al. [25], Jain and Kumar [26], Quan et al. [27] and Ciurte et al. [28]. Hao et al. present a region growing that is performed in a multi-feature vector space. In doing so, they develop three criteria for region growing control: (1.) They use global information instead of local information for the region growing. (2.) They introduce a new idea termed "geographic similarity" to overcome the effects of speckle noise and attenuation artifacts. (3.) They employ an equal opportunity competence criterion to make results independent of processing order.

Bahrami et al. present a boundary delineation for hepatic hemangioma in ultrasound images. Their preprocessing phase includes three main stages: (1.) An image contrast enhancement step, using a so-called Difference of Offset Gaussian (DoOG) approach. (2.) The application of a Canny edge filter. (3.) The application of an adaptive threshold in order to detect the hemangioma ROI.

Finally, a snake algorithm is applied to segment the hemangioma region in the second phase.

Bakas et al. present the semi-automatic segmentation of focal liver lesions in contrast-enhanced ultrasound, which is based on a probabilistic model. Therefore, they propose a two-step method, initialized by a single seed point. In a first step, rectangular force functions are applied to improve the accuracy and computational efficiency of an active ellipse model for approximating the focal liver lesion shape. Afterwards, a probabilistic boundary refinement method is applied to iteratively classify the boundary pixels. Gatos et al. report an automated quantification algorithm for the detection and evaluation of focal liver lesions with contrast-enhanced ultrasound. The lesion detection involves wavelet transform zero crossings utilization as an initialization step to the Markov random field model toward a lesion contour extraction. After the lesion detection across frames, a time intensity curve is computed that provides the contrast agents' behavior at all vascular phases with respect to adjacent parenchyma. From each time intensity curve, eight features were automatically calculated and employed into a support vector machines (SVMs) classification algorithm. Jain and Kumar propose region-difference filters for the segmentation of liver ultrasound images. The region-difference filters evaluate the maximum difference of the average of two regions of the window around the center pixel, which results for a whole image in a region-difference image. Afterwards, the region-difference image was converted into a binary image and morphologically operated for segmenting the desired lesion from the ultrasound image. Quan et al. present the segmentation of tumor ultrasound images via a region-based normalized cut (Ncut) method. In a first step, they use a linear

iterative clustering algorithm to divide the image into a number of homogeneous over-segmented regions. Subsequently, these regions are interpreted as nodes and a similarity matrix is constructed by comparing the histograms of each two regions. In a last step, the Ncut method is applied to merge the over-segmented regions. Ciurte et al. propose a semi-supervised segmentation approach of ultrasound images based on patch representation and continuous Min Cut [29], [30]. Summarized, they use a graph of image patches to represent the ultrasound image and a user-assisted initialization with labels that acts as soft priors and formulate it as a continuous minimum cut problem solved with an optimization algorithm.

II. METHODS

A. Data Acquisition

All images were acquired using a multifrequency-curved probe, which allows ultrasound acquisitions with a bandwith of 1 to 6 MHz (LOGIQ E9/GE Healthcare, Milwaukee, Il, USA and Toshiba Aplio 80, Otawara, Japan). Images of liver metastasis were selected retrospectively from patients with PDAC or NEN in the digital picture archive of the ultrasound unit of the Katharinenhospital Stuttgart (Germany).

B. Measurement

Manual and semi-automatic segmentations were performed by two examiners on a Lenovo Yoga 2 Pro laptop with an Intel Core i7-4500U CPU @ 2.40 GHz, 8 GB RAM and Windows 8.1, 64 bit installed. The two examiners have over 10 years-experience in performing and interpreting US images and performed over 20,000 ultrasound examinations. Besides, the examiners did not know the images, nor have they worked with the algorithm before. In a first session, the examiners manually outlined all metastasis. In addition, they draw the largest diameter (diameter a) and an additional shorter diameter 90 degree related to the first one (diameter b). Time of measurement per metastasis was recorded. In a second session, five weeks later (to decrease bias due to memory effect), the examiners performed the semi-automatic segmentations. Note that the segmentation times have been recorded for every metastasis and the order of the metastasis was randomly redistributed in the second session (semi-automatic segmentation). However, the examiners were instructed in the semi-automatic segmentation with an additional set of ten images of pancreatic cancer liver metastases.

C. Algorithm

The segmentation algorithm has been integrated into the MeVisLab platform, which we used already for various medical applications [31]-[44] and has initially been developed and presented on a limited dataset of liver ultrasound images [45]-[48]. Summarized, the interactive segmentation algorithm

	DSC (%)		HD (Voxel)		Difference Diameter a (mm)		Difference Diameter b (mm)	
	Median	*MAD*	*Median*	*MAD*	*Median*	*MAD*	*Median*	*MAD*
Examiner 1 (n=92)	84	6	9	4	2	2	1	1
Examiner 2 (n=94)	82	7	10	7	3	2	2	2

Table. 1. Summary results of the manual and satisfied semi-automatic measurements for two Internal Medicine specialists (examiner), with Dice Similarity Coefficient (DSC), Hausdorff distance (HD), standard deviation (SAD) and mean absolute deviation (MAD).

needs a user-defined seed point inside the metastasis. Then, the algorithm automatically analyzes the gray values around this seed point like shown in other segmentation tasks [49]-[52], estimating an average gray value of the liver lesion. This makes the algorithm insensitive to different echopattern of homogenous livermasses in ultrasound B-mode, which can appear hyperechoic (brighter), isoechoic (similar) or hypoechoic (darker), when compared to the surrounding liver tissue. Besides, this course of action does not require any parameter changes for different acquisitions. Afterwards, the algorithm generates a specific graph, based on a circular template and performs a minimal s-t-cut. The result of the Min Cut is presented to the user in real-time as a contour outline around the liver lesion. This allows the user to drag the seed point around (inside the lesion) to improve the result until a satisfying segmentation is reached [53]. However, for difficult cases, the user can place additional seeds on the border of the metastasis, which restrict and support the interactive segmentation and was worked already in other structures [54]-[57]. Figure 1 presents the high-level workflow for the semi-automatic segmentation using the so-called US-Cut approach.
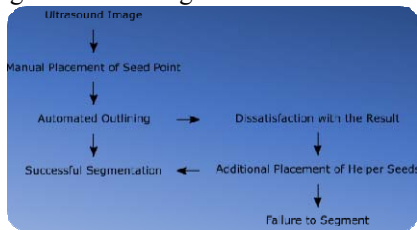

Fig. 1. Workflow of the semi-automatic segmentation approach.

III. RESULTS

For this study, 105 cases (77 ultrasound images of 46 patients diagnosed with PDAC and 28 images of 10 patients with neuroendocrine pancreatic neoplasia) have been used for the evaluation. The median of the maximal lesion diameter was 20 mm and all images displayed liver metastases without overlaying of marker or text. Table 1 presents the summary results of the manual and satisfied semi-automatic measurements for two Internal Medicine specialists (examiner), with the Dice Similarity Coefficient (DSC) [58], the Hausdorff distance (HD) [59], standard deviation (SAD) and mean absolute deviation (MAD). Overall, the examiners were satisfied with the algorithmic segmentation results in 92 (88%) and 94 (90%) cases with the result using the algorithm. However, in seven identical cases, both examiners were not satisfied with the algorithmic segmentation result, even with the support of helper seeds. The Dice score between the manual and semi-automatic segmentations was calculated for each examiner and yielded to a median DSC of 85% for examiner 1 and 82% for examiner 2. In addition, the median HD was calculated, which yielded to a low median distance of 9 pixels for examiner 1 and 10 pixel for examiner 2. Furthermore, the accuracy of the semi-automatic segmentation was analyzed, via the largest diameter (diameter a) with an additional shorter diameter (diameter b) that is 90 degree related to the first one. These were manually drawn by the examiner in addition to the metastasis outline. For the semi-

automatic segmentation, these two diameters were calculated by the algorithm automatically based on the segmentation result. The diameter comparisons (manual / semi-automatic) yielded to a median difference of only 2 mm for diameter a and 1 mm for diameter b for examiner 1, and 3 mm for diameter a and 2 mm for diameter b for examiner 2. For a pure manual segmentation, examiner 1 (n=92) needed median 17.2 seconds, compared to examiner 2 (n=94), who needed median 10.2 seconds. In contrast, a semi-automatic segmentation was in median 7.7 seconds faster when performed by examiner 1 and 2.0 seconds faster when performed by examiner 2.
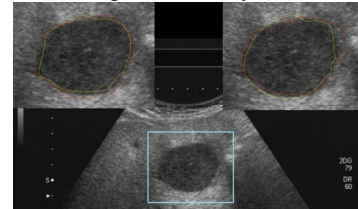

Fig. 2. Segmentation Example marked as adequate by both examiners. Upper left: Segmentation results of examiner 1. Upper right: Segmentation results of examiner 2. Red represent the manual segmentations and yellow represent the semi-automatic segmentations.

For visual inspection, Figure 2 and Figure 3 (left) present segmentation examples marked as adequate by both examiners. Finally, Figure 3 (right) presents a case marked as inadequate by both examiners.
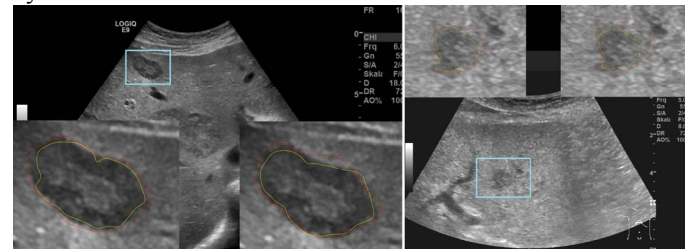

Fig. 3. Segmentation Example marked as adequate (left) and inadequate (right) by both examiners. Lower/Upper left: Segmentation results of examiner 1. Lower/Upper right: Segmentation results of examiner 2. Red represent the manual segmentations and yellow represent the semi-automatic segmentations.

IV. CONCLUSION

In this study, we presented the in-depth assessment of an interactive graph-based approach for the segmentation for pancreatic metastasis in ultrasound acquisitions of the liver. In doing so, two Internal Medicine specialists outlined over one hundred metastases of pancreatic cancer patients manually and with algorithmic support. Besides, the examiners had only a very short training phase of a few minutes to learn the usage of the algorithm. Albeit these challenges, the algorithm performed very well, shortened the segmentation time and could achieve a Dice score of over eighty percent. In addition, the algorithm achieved very small diameter deviations of only one to three millimeters and the examiners were satisfied with the segmentation results in almost ninety percent of the cases. To sum up, highlights of the proposed contribution are as follows: In-depth evaluation of an interactive graph-based approach; Manual outlining of over one hundred datasets by two Internal Medicine specialists; Algorithmic segmentation of the datasets

by the two Internal Medicine specialists; Evaluation via Dice Similarity Coefficient, Hausdorff Distance, lesion diameters and segmentation time; Providing data to the research community. Despite the fact that the study presents encouraging results for a practical application of the algorithm in the clinical routine, there are some limitations that need to be addressed: The study had to be performed retrospectively, because of a missing direct access to the video-output of the ultrasound machine and the inclusion of more than one hundred images of different metastasis. So far, we studied only pancreatic cancer patients, because those are often staged during palliative treatment using abdominal ultrasound combined with endoscopic ultrasound in our clinic.

There are several areas for future work, like – as mentioned before – the direct streaming of the images from the US machines into our software for an immediate segmentation. Further, the enhancement and evaluation of our segmentation method for 3D US images [60]. Finally, providing the segmentation results in an Augmented Reality [61] or Virtual Reality [62] system.

REFERENCES

[1] J. Kleeff, et al., "Pancreatic cancer," Nat. Rev. Dis. Primer 2:16022, 2016.

[2] L. Rahib, et al. "Projecting cancer incidence and deaths to 2030: the unexpected burden of thyroid, liver, and pancreas cancers in the United States," in Cancer Res. 74, 2014, pp. 2913–2921.

[3] M. Hidalgo, "Pancreatic Cancer," N. Engl. J. Med. 362, 2010, pp. 1605–1617.

[4] T. Conroy, et al., "FOLFIRINOX versus gemcitabine for metastatic pancreatic cancer," N. Engl. J. Med. 364, 2011, pp. 1817–1825.

[5] D. D. von Hoff, et al., "Increased survival in pancreatic cancer with nab-paclitaxel plus gemcitabine," in N. Engl. J. Med. 369, 2013, pp. 1691–1703.

[6] T. J. Ettrich, et al., "DocOx (AIO-PK0106): a phase II trial of docetaxel and oxaliplatin as a second line systemic therapy in patients with advanced pancreatic ductal adenocarcinoma," in BMC Cancer 16, 21, 2016.

[7] H. Oettle, et al., "Second-line oxaliplatin, folinic acid, and fluorouracil versus folinic acid and fluorouracil alone for gemcitabine-refractory pancreatic cancer: outcomes from the CONKO-003 trial," in J. Clin. Oncol. off. J. Am. Soc. Clin. Oncol. 32, 2014, pp. 2423–2429.

[8] A. Wang-Gillam, et al., "Nanoliposomal irinotecan with fluorouracil and folinic acid in metastatic pancreatic cancer after previous gemcitabine-based therapy (NAPOLI-1): a global, randomised, open-label, phase 3 trial," in Lancet Lond. Engl. 387, 2016, pp. 545–557.

[9] A. Hann, W. Bohle W, J. Egger, and W. G. Zoller, "Improvement in advanced pancreatic cancer survival with novel chemotherapeutic strategies - experience of a community based hospital," in Z. Gastroenterol. 54, 2016, pp. 1138–1142.

[10] M. Falconi, et al., "ENETS Consensus Guidelines Update for the Management of Patients with Functional Pancreatic Neuroendocrine Tumors and Non-Functional Pancreatic Neuroendocrine Tumors," Neuroendoc. 103, 2016, pp. 153–171.

[11] A. Hann, W. Bohle W, J. Egger, and W. G. Zoller, "Feasibility of alternating induction and maintenance chemotherapy in pancreatic cancer," Sci. Rep. 7, 41549, 2017.

[12] C. P. Pox, and W. Schmiegel, "[German S3-guideline colorectal carcinoma]," Dtsch. Med. Wochenschr. 1946 138, 2545, 2013.

[13] T. Seufferlein, J. B. Bachet, E. Van Cutsem, P. Rougier, and ESMO Guidelines Working Group, "Pancreatic adenocarcinoma: ESMO-ESDO Clinical Practice Guidelines for diagnosis, treatment and follow-up," in Ann. Oncol. Off. J. Eur. Soc. Med. Oncol. ESMO 23 Suppl 7, vii, 2012 pp. 33–40.

[14] C. J. Harvey, and T. Albrecht, "Ultrasound of focal liver lesions," in Eur. Radiol. 11, 2001, pp. 1578–1593.

[15] J. Hohmann, et al., "Characterisation of focal liver lesions with unenhanced and contrast enhanced low MI real time ultrasound: on-site unblinded versus off-site blinded reading," in Eur. J. Radiol. 81, 2012, e317–324.

[16] J. Egger, et al., "GBM Volumetry using the 3D Slicer Medical Image Computing Platform," Sci Rep. 3, 1364, 2013.

[17] D. Zukić, et al. "Robust Detection and Segmentation for Diagnosis of Vertebral Diseases using Routine MR Images," Computer Graphics Forum, Volume 33(6), pp. 190-204, 2014.

[18] D. Zukic, et al., "Segmentation of Vertebral Bodies in MR Images," Vision, Modeling, and Vis., pp. 135-142, 2012.

[19] J. Egger, et al., "Aorta Segmentation for Stent Simulation," Cardiovascular Interventional Imaging and Biophysical Modelling Workshop, MICCAI, pp. 1-10, 2009.

[20] J. Egger, T. O'Donnell, C. Hopfgartner, and B. Freisleben, "Graph-Based Tracking Method for Aortic Thrombus Segmentation," MBEC, Springer, pp. 584-587, 2008.

[21] J. Egger, T. Kapur, C. Nimsky, and R. Kikinis, "Pituitary Adenoma Volumetry with 3D Slicer," PLoS ONE 7, e51788, 2012.

[22] X. Hao, C. Bruce, C. Pislaru, and J. F. Greenleaf, "A novel region growing method for segmenting ultrasound images," in Ultrasonics Symposium, 2000, pp. 1717–1720.

[23] N. Bahrami, S. H. Rezatofighi, A. M. Adeli, and S. K. Setarehdan, "Boundary delineation for hepatic hemangioma in ultrasound images," in Conf. Proc. Annu. Int. Conf. IEEE Eng. Med. Biol. Soc., 2011, pp. 7989–7992.

[24] S. Bakas, et al., "Fast semi-automatic segmentation of focal liver lesions in contrast-enhanced ultrasound, based on a probabilistic model," in Computer Methods in Biomechanics and Biomedical Engineering. 2015, pp. 1–10.

[25] I. Gatos, et al., "A new automated quantification algorithm for the detection and evaluation of focal liver lesions with contrast-

enhanced ultrasound: Focal liver lesions and contrast-enhanced ultrasound," in Med. Phys. 42, 2015, pp. 3948–3959.

[26] N. Jain, and V. Kumar, "Liver Ultrasound Image Segmentation Using Region-Difference Filters," J. Digit. Img. 2016, pp. 1–15.

[27] L. Quan, D. Zhang, Y. Yang, Y. Liu, and Q. Qin, "Segmentation of tumor ultrasound image via region-based Ncut method," in Wuhan Univ. J. Nat. Sci. 18(4), 2013, pp. 313–318.

[28] A. Ciurte, et al. "Semi-supervised segmentation of ultrasound images based on patch representation and continuous min cut," in PloS One 9, 2014, e100972.

[29] Y. Boykov, and V. Kolmogorov, "An Experimental Comparison of Min-Cut/Max-Flow Algorithms for Energy Minimization in Vision," IEEE PAMI 26, pp. 1124-1137, 2004.

[30] J. Egger, "PCG-Cut: Graph Driven Segmentation of the Prostate Central Gland," PLoS One 8, e76645, 2013.

[31] J. Egger, et al., "Integration of the OpenIGTLink network protocol for image-guided therapy with the medical platform MeVisLab," in Int. J. Med. Robot. Comput. Assist. Surg. MRCAS 8, 2012. pp. 282–290.

[32] K. Greiner, et al., "Segmentation of Aortic Aneurysms in CTA Images the Statistic Approach of the Active Appearance Models," Proceedings of Bildverarbeitung für die Medizin (BVM), Berlin, Germany, Springer Press, pp. 51-55, 2008.

[33] J. Lu, J. Egger, A. Wimmer, S. Großkopf, and B. Freisleben, "Detection and Visualization of Endoleaks in CT Data for Monitoring of Thoracic and Abdominal Aortic Aneurysm Stents," SPIE Med Img 6918, 69181F(1-7), 2008.

[34] J. Egger, Z. Mostarkic, S. Grosskopf, and B. Freisleben, "A Fast Vessel Centerline Extraction Algorithm for Catheter Simulation," CBMS, pp. 177-182, IEEE Press, June 2007.

[35] J. Egger, S. Grosskopf, C. Nimsky, T. Kapur, and B. Freisleben, "Modeling and Visualization Techniques for Virtual Stenting of Aneurysms and Stenoses," Comput Med Imaging Graph., 36(3):183-203, 2012.

[36] J. Klein, et al., "On the Reliability of Diffusion Neuroimaging," Neuroimaging, Sciyo, 1-24, ISBN 978-953-307-127-5, 2010.

[37] T. Lüddemann, and J. Egger, "Iterative-cuts: longitudinal and scale-invariant segmentation via user-defined templates for rectosigmoid colon in gynecological brachytherapy," J Med Imaging (Bellingham), 3(2):024004, April 2016.

[38] R. D. Renapurkar, et al., "Aortic volume as an indicator of disease progression in patients with untreated infrarenal abdominal aneurysm," Eur J Radiol., 81(2):e87-93, 2011.

[39] J. Egger, et al., "Fast Self-Collision Detection and Simulation of Bifurcated Stents to Treat Abdominal Aortic Aneurysms (AAA)," 29th Ann. Int. Conf. of the IEEE Engineering in Medicine and Biol. Society, Lyon, France, pp. 6231-6234, 2007.

[40] J. Egger, Z. Mostarki, S. Grosskopf, and B. Freisleben, "Preoperative Measurement of Aneurysms and Stenosis and Stent-Simulation for Endovascular Treatment," ISBI, pp. 392-5, 2007.

[41] J. Egger, S. Grosskopf, and B. Freisleben, "Simulation of Bifurcated Stent Grafts to Treat Abdominal Aortic Aneurysms (AAA)," SPIE, 6509, 1-6, 2007.

[42] M. H. A. Bauer, et al., "A fast and robust graph-based approach for boundary estimation of fiber bundles relying on fractional anisotropy maps," 20th International Conference on Pattern Recognition (ICPR), Istanbul, Turkey. IEEE Computer Society, Los Alamitos, 4016-4019, 2010.

[43] D. Kuhnt, et al., "Fiber tractography based on diffusion tensor imaging (DTI) compared with High Angular Resolution Diffusion Imaging (HARDI) with compressed sensing (CS) – initial experience and clinical impact," Neurosurgery, Volume 72, pp. A165-A175, 2013.

[44] M. H. A. Bauer, et al., "Boundary Estimation of Fiber Bundles derived from Diffusion Tensor Images," Int J CARS, 6(1):1-11, 2011.

[45] J. Egger, et al., "US-Cut: interactive algorithm for rapid detection and segmentation of liver tumors in ultrasound acquisitions," in SPIE Medical Imaging, 97901C, 2016.

[46] J. Egger, D. Schmalstieg, X. Chen, W. G. Zoller, and A. Hann, "Interactive Outlining of Pancreatic Cancer Liver Metastases in Ultrasound Images," in Sci. Rep. 7, 892, 2017.

[47] J. Egger, et al., "RFA-Cut: Semi-automatic Segmentation of Radiofrequency Ablation Zones with and without Needles via Optimal s-t-Cuts," in IEEE EMBC, pp. 2423–2429, 2015.

[48] J. Egger, et al., "Interactive Volumetry of Liver Ablation Zones," in Sci. Rep. 5, 15373, 2015.

[49] R. Schwarzenberg, B. Freisleben, C. Nimsky, and J. Egger, "Cube-Cut: Vertebral Body Segmentation in MRI-Data through Cubic-Shaped Divergences," PLoS One, 9(4):e93389, 2014.

[50] J. Egger, et al., "Square-Cut: A Segmentation Algorithm on the Basis of a Rectangle Shape," PLoS One, 7(2):e31064, 2012.

[51] J. Egger, M. H. A. Bauer, D. Kuhnt, B. Freisleben, and C. Nimsky, "Pituitary Adenoma Segmentation", Proc. of Inter. Biosignal Processing Conf., Paper-ID 061, pp. 1-4, 2010.

[52] J. Egger, B. Freisleben, C. Nimsky, and T. Kapur, "Template-Cut: A Pattern-Based Segmentation Paradigm," Sci Rep., Nature Publishing Group (NPG), 2:420, 2012.

[53] J. Egger, T. Lüddemann, R. Schwarzenberg, B. Freisleben, and C. Nimsky, "Interactive-Cut: Real-Time Feedback Segmentation for Translational Research," Comp Med Imaging Graph 38, pp. 285-95, 2014.

[54] J. Egger, "Refinement-Cut: User-Guided Segmentation Algorithm for Translational Science," Sci. Rep. 4, 5164, 2014.

[55] J. Egger, R. R. Colen, B. Freisleben, and C. Nimsky, "Manual Refinement System for Graph-Based Segmentation Results in the Medical Domain" J Med Syst. 36, pp. 2829-39, 2012.

[56] J. Egger, C. Kappus, B. Freisleben, and C. Nimsky, "A Medical Software System for Volumetric Analysis of Cerebral Pathologies in Magnetic Resonance Imaging (MRI) Data," J Med Syst., 36(4):2097-109, 2011.

[57] J. Egger, et al., "A Flexible Semi-Automatic Approach for Glioblastoma multiforme Segmentation," Biosignal:1-4, 2010.

[58] L. R. Dice, "Measures of the Amount of Ecologic Association Between Species," in Ecology 26, 1945, pp. 297–302.

[59] D. P. Huttenlocher, G. A. Klanderman, and W. A. Rucklidge, "Comparing images using the Hausdorff distance," in IEEE PAMI. 15, 1993, pp. 850–863.

[60] J. Egger, et al. "Nugget-Cut: A Segmentation Scheme for Spherically- and Elliptically-Shaped 3D Objects," in DAGM, 2010, pp. 373–382.

[61] X. Chen, et al. "Development of a surgical navigation system based on augmented reality using an optical see-through head-mounted display," in J. Biomed. Inform. 55, 2015, pp. 124–131.

[62] J. Egger, et al. "HTC Vive MeVisLab integration via OpenVR for medical applications," in PLoS ONE 12(3): e0173972, 2017.